Dielectric Study of Terminal Chain Dynamics, Segmental Motion, and Rotation of Side Groups in Polyethers of Type ABC

Minoru Yamane, Yuji Hirose,† and Keiichiro Adachi*

Department of Macromolecular Science, Graduate School of Science, Osaka University, Toyonaka, Osaka 560-0043, Japan

Received August 15, 2005; Revised Manuscript Received October 6, 2005

ABSTRACT: Dielectric measurements were carried out on undiluted poly(isopropyl glycidyl ether) (PiPGE), poly(*n*-butyl glycidyl ether) (PnBGE), and poly(*tert*-butyl glycidyl ether) (PtBGE) which have dipoles aligned parallel (type A) and perpendicular (type B) to the chain contour and the dipoles residing on the flexible side group (type C). These polyethers exhibited three dielectric relaxations designated as α_n, α_s, and β. The α_n relaxation is due to the normal mode relaxation. The primary α_s relaxation is assigned to local segmental motions coupled with rotation of the side group. The β relaxation can be assigned to both twisting motions of the main chain and libration of the side groups of a small amplitude. Independent full rotation of the side groups was not observed below T_g. The relaxation strengths and dipole moments associated with the α_n, α_s, and β processes have been estimated. In PiPGE and PtBGE, the temperature dependence of the loss maximum frequency f_{ms} for the α_s relaxation was much steeper than that f_{mn} for the normal mode, and $\log(f_{ms}/f_{mn})$ increased with temperature. On the other hand, $\log(f_{ms}/f_{mn})$ for PnBGE was almost independent of temperature.

Introduction

Dielectric normal mode spectroscopy has been used to investigate terminal chain dynamics and chain dimension in various complex systems.[1−6] Polyethers having chemical structure of $-(CH_2-CHR-O-)_n$ such as poly(propylene oxide) (PPO, R = CH_3) is known to be a group of type AB polymer having the components of the dipole moment aligned in the parallel (type A) and transverse (type B) directions with respect to the chain contour.[7−17] Recently, Casalini and Roland reported the dielectric relaxation of poly(butylene oxide) (PBO, R = CH_3CH_2) under high pressure.[15] We also reported the dielectric properties of PBO and poly(styrene oxide) (PSO, R = C_6H_5) and found that the former exhibits clearly the normal mode relaxation, but the latter does not.[16,17] This indicates that the dielectric normal modes of polyethers depend strongly on the chemical structure of the side group. Comparing these polyethers, we also notice that the local segmental dynamics depends strongly on the side group, namely the glass transition temperatures T_g of PPO, PBO, and PSO are 200, 199, and 310 K, respectively.[10,16,17] Those polyethers so far studied have relatively nonpolar side groups. In this study we aim to investigate the effect of a polar side group on the dielectric behavior. For this purpose we used three kinds of poly(alkyl glycidyl ether)s having the side group R = $-CH_2-O-R'$, namely, poly(isopropyl glycidyl ether) (PiPGE, R′ = $-CH(CH_3)_2$), poly(*n*-butyl glycidyl ether) (PnBGE, R′ = $-(CH_2)_3-CH_3$), and poly(*tert*-butyl glycidyl ether) (PtBGE, R′ = $-C(CH_3)_3$).

It is expected that these polyethers exhibit dielectric relaxations due to rotation of the side group. The dipoles residing on flexible side groups are classified as type C according to the classification of Stockmayer.[1] Therefore, these polyethers belong to type ABC polymers. So far only one group of polymers, i.e., poly(organo phosphazene)s, are known as a type ABC polymer.[18] Uzaki et al. reported the dielectric behavior of undiluted poly(phenoxyphosphazene).[19] However, the polymer is a crystalline polymer, and furthermore it forms a mesophase in the molten state. No dielectric behavior of a perfectly amorphous type ABC polymer has been reported. In this study we will also focus on the dielectric relaxation caused by the type C dipoles. We will discuss the relationship between segmental motions and rotation of the side groups in conjunction with the recent issue of dynamical heterogeneity in miscible blends.[20]

Experimental Section

Materials. PiPGE, PnBGE, and PtBGE were prepared by ring-opening polymerization of corresponding epoxides by using potassium hydride as the initiator and 18-crown-6 as the catalyst in tetrahydrofuran.[21] All those reagents were purchased from Aldrich. Typical conditions of synthesis were as follows: 5 g of potassium hydride was suspended in 100 mL of dry tetrahydrofuran, and then 5 g of 18-crown-6 and 25 mL of the epoxide were added and stirred overnight at about 295 K. Polymerization was terminated by adding methanol slowly. Weight-average molecular weight (M_w) and polydispersity index (M_w/M_n) were determined by a gel permeation chromatograph (GPC) equipped with a light scattering detector (Tosoh LS 8000, Japan). Sample characteristics are shown in Table 1. The samples are amorphous, and no crystallization was observed by calorimetry.

Methods. The glass transition temperature T_g was determined by a differential scanning calorimeter (Seiko Instruments & Electronics Ltd., DSC-20, Japan) at a heating rate of 10 K/min and listed in Table 1. Measurements of the relative dielectric constant ϵ' and the dielectric loss factor ϵ'' were made by using RLC meters (QuadTech, models 1693 and 7600) in the frequency range from 10 Hz to 2 MHz. Measurements were made automatically with a four terminal circuit with the GPIB (IEE-488) system. Before measurements, the capacitance and the dissipation factor (tan δ) of a standard capacitance were measured at all frequencies and recorded in a personal computer for calibration of the capacitance and the null point of the dissipation factor. Measurements were made in the

† Present address: Venture Business Lab., Chiba University, Inage, Chiba 263-8522, Japan.

* To whom correspondence should be addressed. E-mail: adachi@chem.sci.osaka-u.ac.jp.

10.1021/ma051796v CCC: $30.25
Published on Web 11/12/2005

Table 1. Weight-Average Molecular Weight M_w, Polydispersity Index M_w/M_n, and Glass Transition Temperature T_g of Poly(alkyl glycidyl ether)s

code	$10^{-3}M_w$	M_w/M_n	T_g
PiPGE-22	22	1.55	206
PnBGE-25	25	1.49	194
PtBGE-21	21	1.57	249
PtBGE-37	37	1.79	249

continuously heating mode with a heating rate of about 0.2 K/min. The frequency f dependences of ϵ' and ϵ'' at fixed temperatures T were calculated automatically with the personal computer by interpolation of ϵ' and ϵ'' using sets of the $\epsilon'(f,T) - \epsilon''(f,T)$ data. The capacitance cell for measurements of viscous liquids was reported previously, and the cryostat has been modified into the four-terminal connection.[22]

In some samples ϵ'' increased in the low-frequency region due to contamination of impurity ions. We corrected the contribution ϵ_σ'' of the ionic conductivity σ by subtracting ϵ_σ'' from the observed value of ϵ'':

$$\epsilon_\sigma'' = \frac{\sigma}{2\pi\epsilon_0 f} \tag{1}$$

where ϵ_0 is the absolute dielectric constant of vacuum and f the frequency in hertz. First σ was estimated by assuming that ϵ'' at the lowest frequency (10 Hz) was totally due to the ionic conduction. Then a slightly smaller value than the thus-estimated σ was used in calculation of eq 1 to avoid overestimation of σ.

Results and Discussion

Temperature and Frequency Dependences of ϵ' and ϵ''. a. PiPGE. Figure 1 shows the temperature dependences of ϵ' and ϵ'' for PiPGE-22. Two loss peaks seen above 200 K are designated as α_n and α_s from the high-temperature side. The ϵ' and ϵ'' curves seen in Figure 1 are very similar to those of poly(butylene oxide) (PBO) in which the high-temperature peak shifted to high temperature with increasing molecular weight

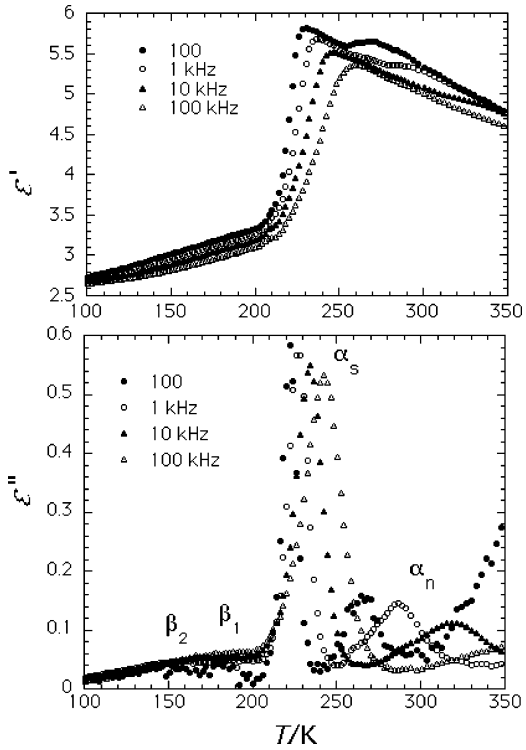

Figure 1. Temperature dependences of ϵ' (top) and ϵ'' (bottom) for PiPGE-22.

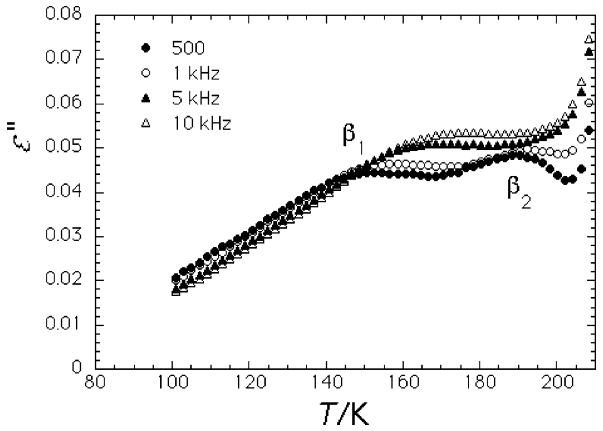

Figure 2. Temperature dependence of ϵ'' of PiPGE in the temperature range of below T_g.

(MW), and hence the high-temperature peak of PBO was assigned to the normal mode.[16] Although we have not examined the MW dependence of the ϵ'' curve for PiPGE, the α_n peak is assigned to the normal mode. As described later, PtBGE also exhibits the same behavior as PBO, indicating that the α_n process in poly(alkyl glycidyl ether)s can be assigned to the normal mode. On the other hand, the α_s peak can be assigned to the primary relaxation since this peak is observed ca. 20−30 K above the glass transition temperature (T_g = 206 K). Below T_g, a small loss peak is seen around 160 K. Figure 2 shows the magnification of this region. There are two loss peaks in this region, and they are designated as β_1 and β_2. The mechanisms of the secondary relaxations will be discussed later.

Figure 3a,b shows the frequency dependences of ϵ'' of PiPGE-22 at various temperatures. The loss curves seen in Figure 3a are due to the α_s relaxation and those in Figure 3b to the α_n relaxation. The increase of ϵ'' in the low-frequency region is due to ionic conduction, but the contribution was relatively weak and the correction of eq 1 was not necessary for the data shown in Figure 3a. Figure 3b shows the ϵ'' curves in the region where the normal mode relaxation occurs. In this high-temperature region, the correction of eq 1 was made, but ϵ'' still increases in the low-frequency region due to imperfect corrections of σ, as described in the Experimental Section.

In Figure 3a, we note that the shape of the ϵ'' curve is abnormal; i.e., as seen for the ϵ'' curve at 224 K, the ϵ'' curve in the high-frequency region becomes almost flat, indicating the existence of a distinct relaxation process. To assign this satellite loss peak, we plotted the loss maximum frequencies f_m for the α_s, β_1, and β_2 relaxations with respect to inverse of temperature in Figure 4, where we see that these relaxations merge around 10 MHz and $1000/T = 3.7$ (T = 270 K). As discussed later, the β_1 and β_2 relaxations can be assigned to libration of the side group and local twisting motion of the main chain. We also note in Figure 2 that the intensities of the β_1 and β_2 relaxations increase rapidly with increasing temperature probably due to increase of the amplitude of the libaration of the side group. Thus, we conclude that the α_s relaxation of PiPGE is due to both of the local segmental motions of the main chain and rotation of the side group.

b. PnBGE. Figure 5 shows the temperature dependences of ϵ' and ϵ'' of poly(*n*-butyl glycidyl ether) (PnBGE-25). Figure 6 shows the ϵ'' vs temperature curves below

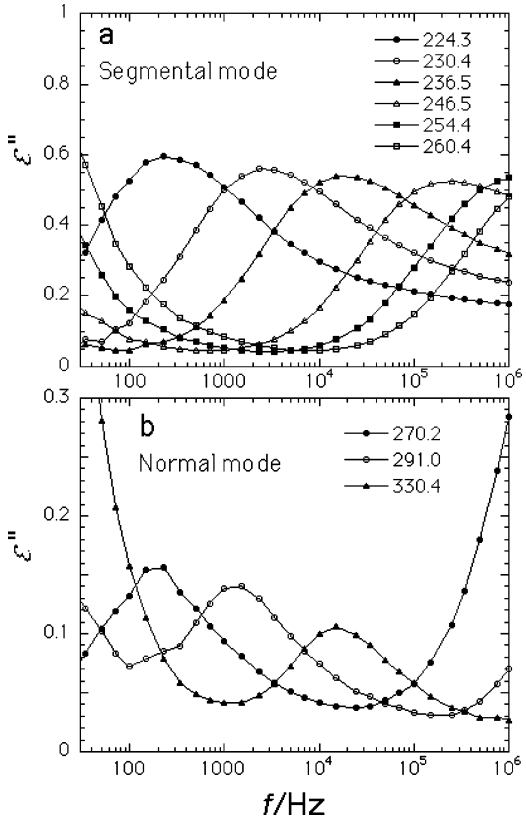

Figure 3. Frequency dependence of ϵ'' of PiPGE-22 in (a) the α_s relaxation region and (b) the α_n relaxation region.

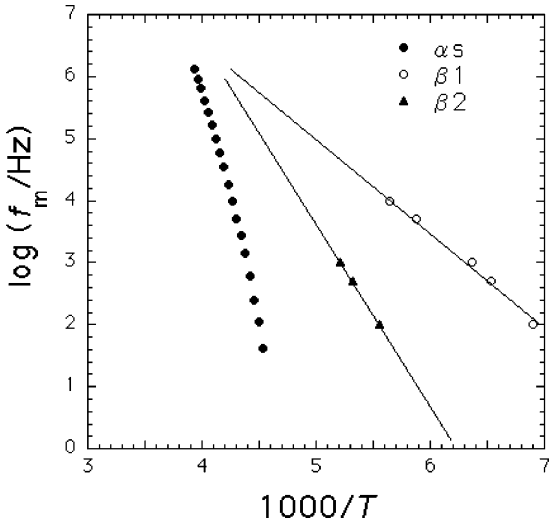

Figure 4. Arrhenius plots of loss maximum frequencies f_m for the α_s, β_1, and β_2 relaxations of PiPGE.

T_g (=194 K). Similar behavior to PiPGE can be seen in Figure 5, but as seen in Figure 6 the ϵ'' curve below T_g is unimodal in contrast to PiPGE. The loss peaks are designated as the α_n, α_s, and β relaxations as indicated in the figure and can be assigned to the normal mode relaxation, the primary relaxation, and the secondary relaxation, respectively. As shown in Figure 6, the intensity of the β relaxation increases with increasing temperature probably due to increase of the amplitude of libration of the side group.

Figure 7 shows the frequency dependences of ϵ'' of PnBGE-25 in the temperature regions where the α_s relaxation (a) and the α_n relaxation (b) are seen. In both regions, the correction of eq 1 was not made. As seen in

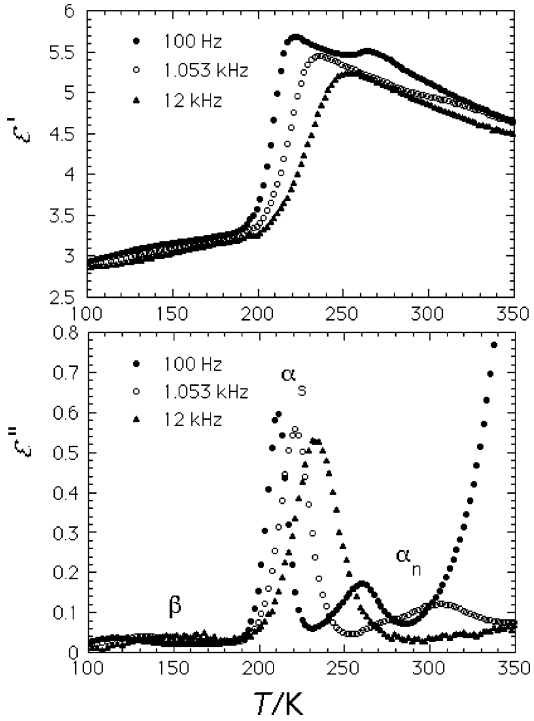

Figure 5. Temperature dependences of ϵ' (top) and ϵ'' (bottom) of PnBGE-25.

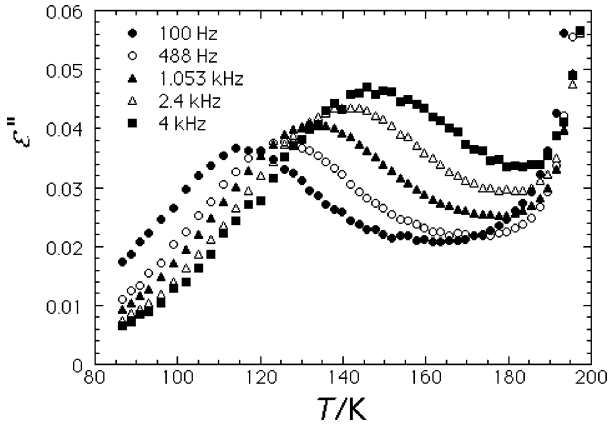

Figure 6. Temperature dependence of ϵ'' of PnBGE in the temperature range below T_g.

Figure 7a, the ϵ'' curve at 205.4 K exhibits the relatively high intensity of ϵ'' in the high-frequency region, indicating the existence of a satellite relaxation process around 10^5 Hz as observed for PiPGE in Figure 2a. The relaxation process is attributed to the β process (see Figure 14). We note that the intensity of the overlapped β relaxation is low at 205 K, but we expect that it increases rapidly with increasing temperature.

c. PtBGE. Figure 8 shows the temperature dependences of ϵ' (top) and ϵ'' (bottom) for PtBGE-21. Figure 9 shows the ϵ'' curves in the β relaxation region. The frequency dependence of ϵ'' of PtBGE-21 is shown in Figure 10a,b. We see in these figures that the dielectric behaviors of the α_n, α_s, and β relaxations of PtPGE are similar to those of PiPGE and PnBGE. Therefore, the assigments of these relaxation processes are the same as PiPGE and PnBGE. In Figure 10a, the merging of the segmental relaxation and the β relaxation is most clearly seen in the ϵ'' curves at 245 and 251 K; i.e., ϵ'' increases around 10^6 Hz, indicating the existence of the β relaxation around 10^7 Hz. The separation between the

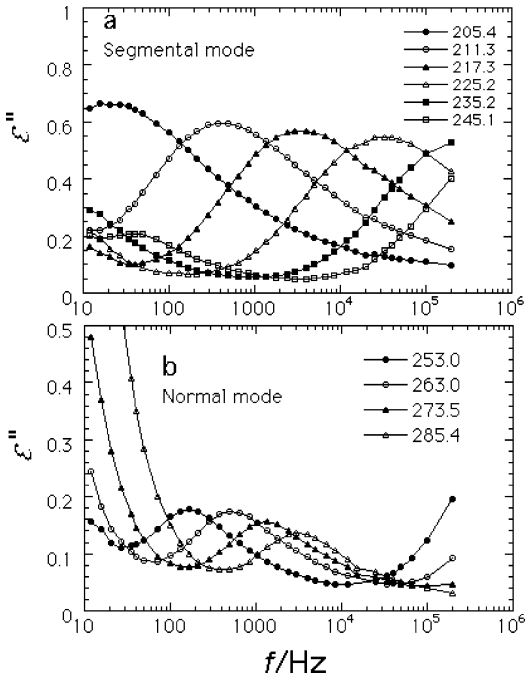

Figure 7. Frequency dependences of ϵ'' of PnPGE-25 in (a) segmental mode region and (b) the normal mode region.

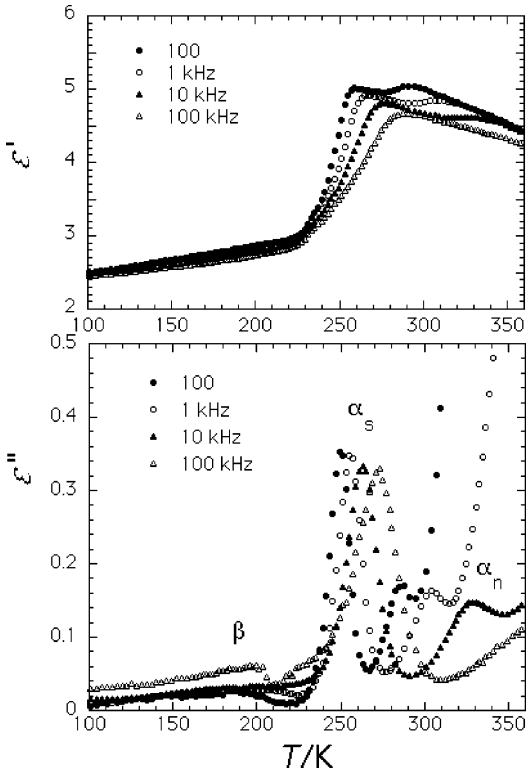

Figure 8. Temperature dependence of ϵ' (top) and ϵ'' (bottom) of PtBGE-21.

α_s and β relaxations becomes narrow with increasing temperature, and the ϵ'' curve at 275 K exhibits a flat loss peak which indicates that two loss peaks having similar intensities and slightly different loss maximum frequency are overlapped. We expect that above 275 K the segmental mode and the rotation of the side group are completely coupled.

For PtBGE we carried out measurements on samples with different MW. Figure 11 shows the frequency dependences of ϵ'' of PtBGE-37 in the segmental (a) and

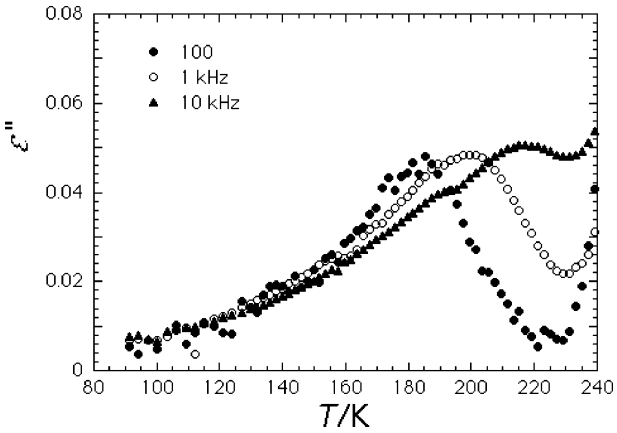

Figure 9. Temperature dependence of ϵ'' of PtBGE-21 in the temperature range below T_g.

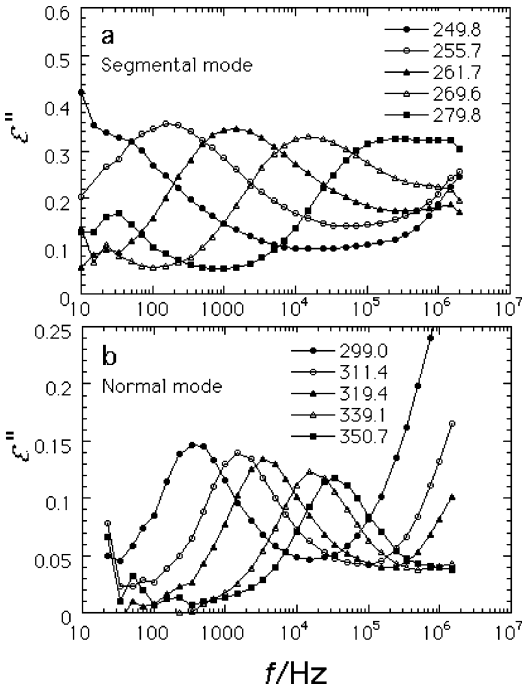

Figure 10. Frequency dependence of ϵ'' in (a) the segmental mode region and (b) normal mode region for PtPGE-21.

normal mode (b) regions. Comparing Figures 10 and 11, we see that the ϵ'' curve for the normal mode shifts to low frequency with increasing MW. This confirms the assignment of the α_n relaxation. Although not shown here, PtBGE-37 exhibited similar temperature dependences of ϵ' and ϵ'' to PtBGE-21. In our recent paper,[16] it was found that the characteristic molecular weight M_c of poly(butylenes oxide) (PBO) is ca. 6000, and above M_c the normal mode relaxation time τ_n of PBO is proportional to $M^{3.4}$. From the ratio of the loss maximum frequencies f_m for the normal modes of PtBGE-37 and PtBGE-21, τ_n of PtBGE is approximately proportional to $M^{3.4}$. Although this power includes a large error arising from the error in determination of MW, we see that MW dependence of τ_n of PtBGE is similar to PBO.

It is seen in Figures 3, 7, and 10 that the loss curves for the normal mode are narrow and the half-width is about 1.5 decades. Both the Rouse model[23] for unentangled chain dynamics and the tube model[24,25] for entangled chain dynamics predict the common width of 1.27 decades. The half-width for the Debye theory is 1.14

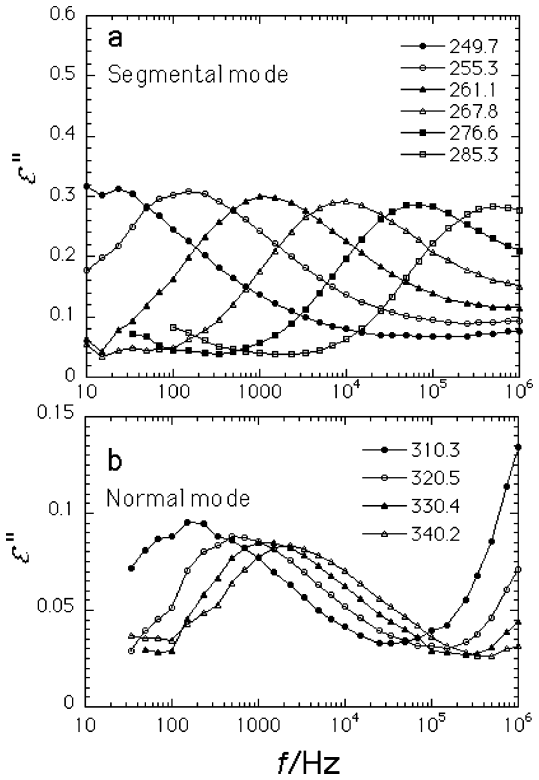

Figure 11. Frequency dependence of ϵ'' in (a) the segmental mode region and (b) normal mode region for PtPGE-37.

Table 2. Relaxation Strengths for the Segmental Mode $\Delta\epsilon_s$, Relaxation Strengths for the Normal Mode $\Delta\epsilon_n$, Effective Dipole Moment $g^{1/2}p_B$ per Monomer Unit for the Segmental Mode, Dipole Moment p_A per Monomer Unit for the Normal Mode, and the Dipole Moment μ per Unit Contour Length[a]

	segmental mode			normal mode			
code	T/K	$\Delta\epsilon_s$	$g^{1/2}p_B$/D	T/K	$\Delta\epsilon_n$	p_A/D	$10^{11}\mu$/esu
PPO-3[b]	220	3.05	0.82	236	0.52	0.39	1.10
PSO-12[c]	330	1.08	0.72	370	0.00	0.00	0.00
PBO-21[d]	221	1.93	0.79	320	0.74	0.59	1.65
PiPGE-22	224	2.19	1.21	300	0.37	(0.39)	(1.1)[e]
PnBGE-25	217	2.19	1.08	285	0.39	(0.43)	(1.2)
PtPGE-21	259	1.58	1.18	315	0.39	(0.46)	(1.3)

[a] 1 D = 10^{-18} esu·cm = 3.336 × 10^{-30} C·m. [b] Reference 10. [c] Reference 17. [d] Reference 16. [e] Estimated (see text).

decades. The observed widths of the normal modes are broader than the theories mainly due to distribution of MW. We also note that the width for the normal mode of PtBGE-37 is broader than that of PtBGE-21. Obviously this is due to the broader MW distribution of PtBGE-37 with $M_w/M_n = 1.79$ than that of PtBGE-21 with $M_w/M_n = 1.57$.

Relaxation Strength and Dipole Moment. The relaxation strengths for the segmental mode $\Delta\epsilon_s$ and those for the normal mode $\Delta\epsilon_n$ have been determined by using Cole−Cole plots and are listed in Table 2. For the sake of comparison, the relaxation strengths for poly(propylene oxide) (PPO),[10] poly(styrene oxide) (PSO),[17] and poly(butylene oxide) (PBO)[16] are also listed. Since the α_s and β relaxations merge in the temperature region above T_g, the Cole−Cole plot for the α_s relaxation exhibits a shape that two semicircles are overlapped. Therefore, the relaxation strength for the α_s process includes the contributions of both segmental motion of the main chain and rotation of the side group.

The dipole moment for the α_s relaxation was calculated with the Onsager−Kirkwood equation (in cgs esu units):[26,27]

$$\Delta\epsilon = \frac{4\pi N g {p_B}^2}{3k_B T}\frac{(\epsilon_U + 2)^2\epsilon_R}{3(2\epsilon_R + \epsilon_U)} \tag{2}$$

where N is the number of the monomer unit in unit volume, g the Kirkwood correlation parameter, and p_B the type B dipole moment of the monomer unit. Here it is noted that p_B of the three poly(alkyl glycidyl ether)s used in the present study is a statistical average of the dipole vector of the ether group of the main chain and that of the side group. The side group takes several energetically stable conformations through internal rotation of the bonds. The average conformation of the side group determines p_B.

From the data of $\Delta\epsilon$, $g^{1/2}p_B$ is determined and listed in Table 2. Here we assumed that the densities are 1.0 g/cm^3. It is seen that the values of $g^{1/2}p_B$ of poly(alkyl glycidyl ether)s used in this study are larger than those of PPO, PSO, and PBO reflecting the contribution of the polar side groups. In the case of PPO, PSO, and PBO the dipoles reside only on the backbone. In this case dipole−dipole interactions occur mainly through intramolecular interactions among the neigboring monomer units. Previously, we estimated g for PBO to be 0.87.[16] In poly(alkyl glycidyl ether)s, the dipolar interactions also occur through intramolecular interactions, especially between the side group and the backbone dipoles in the same monomer unit.

The relaxation strength $\Delta\epsilon_n$ for the normal mode of undiluted polymers is given by[2]

$$\frac{\Delta\epsilon_n}{\rho} = \frac{4\pi N_A \mu^2 \langle r^2\rangle}{3k_B TM} \tag{3}$$

where ρ is the density in the unit of g/mL, μ the dipole moment per unit contour length, and $\langle r^2\rangle$ the mean-square end-to-end distance. Here we have assumed that the internal field factor is unity.[2] To determine μ, the data of $\langle r^2\rangle$ are necessary. Unfortunately, $\langle r^2\rangle$ for poly(alkyl glycidyl ether) are not available. Therefore, we have estimated roughly the parallel dipole moment μ per unit contour length, assuming that the characteristic ratios C_∞ of poly(alkyl glycidyl ether)s are the same as that of PBO ($C_\infty = 5.7 \pm 0.2$).[28] It is noted that C_∞ of most polymers is in the range of 6 ± 2.[29] Therefore, the error of the estimation of $\langle r^2\rangle/M$ may be within 30%. The results are listed in Table 2. It is seen that the parallel dipole moment p_A of polyether depends strongly on the chemical structure of side group. The backbone of polyethers is represented as $-C^1-O-C^2-$ where C^1 is the carbon atom on which the side group R is attached and C^2 is the carbon atom of the methylene group. The electronic affinity of R results in the difference in the electronic density between C^1 and C^2, and hence the parallel dipole moment is formed. In the case of PSO the distribution of electrons between of C^1 and C^2 becomes almost symmetrical, and hence p_A becomes zero.

If the dipole on the side group of poly(alkyl glycidyl ether) takes a statistically favored orientation with respect to the main chain, p_A is determined by the sum of the dipole vectors on the main chain and the side group. Smaller p_A of poly(alkyl glycidyl ether) than that of PBO may be partly due to such an effect.

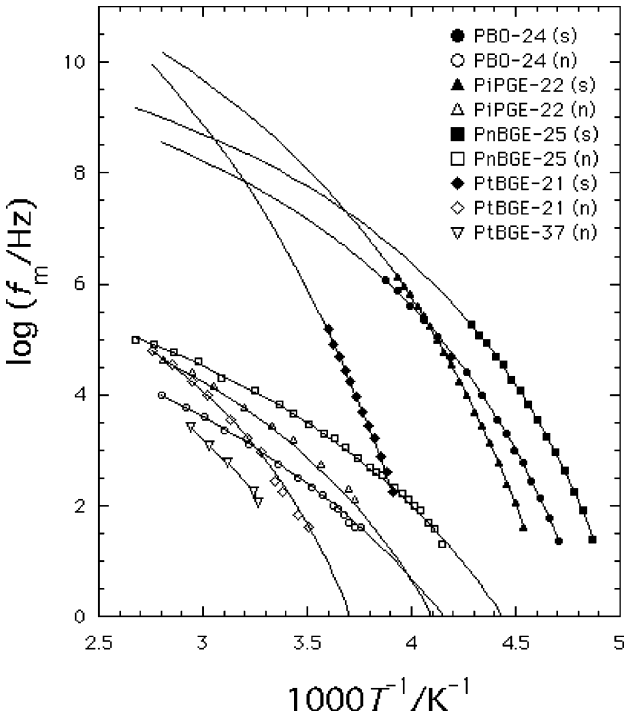

Figure 12. Arrhenius plots of loss maximum frequencies for the segmental mode f_{ms} and those for the normal mode f_{mn}. In the sample codes, (n) and (s) indicate the normal and segmental modes, respectively.

Table 3. Parameters of the Vogel −Fulcher Equation for the Segmental and Normal Modes

	segmental mode			normal mode		
code	A	B	T_0	A	B	T_0
PBO-24	10.9	448	165.5	6.9	572	157.5
PiPGE-22	13.9	729	161.0	7.2	455	181.0
PnBGE-25	11.2	421	162.1	7.2	459	161.7
PtBGE-21	15.7	1078	171.5	8.02	499	202.8

Temperature Dependences of the Loss Maximum Frequencies for Segmental and Normal Modes. The temperature dependences of the loss maximum frequencies for the segmental mode f_{ms} and normal modes f_{mn} are plotted against the inverse of temperature in Figure 12. For the sake of comparison, log f_{mn} and log f_{ms} for PBO are also plotted. Those plots are fitted to the Vogel−Fulcher equation:[30,31]

$$\log f_m = A - \frac{B}{T - T_0} \tag{4}$$

where A, B, and T_0 are the parameters. The fitting curves are indicated by the solid lines, and the values of the parameters are listed in Table 3.

It is seen that the average slopes of the nonlinear Arrhenius plots for the segmental modes of PiPGE and PtBGE are higher than those of PBO and PnBGE. This is reflected on the values of A and B; i.e., the average slope increases with increasing A and B. Especially the value of B for the segmental mode of PtBGE is high. Similar behavior was observed previously for poly(*n*-butyl acrylate), which exhibited B as high as 1620.[32] The fragility m is used frequently for comparison of the slope of the Arrhenius plot.[33] However, we cannot use m in the present analyses since it is defined as the slope at $T = T_g$, at which the relaxation frequency becomes ca. 0.001 Hz: extrapolation of the Arrhenius plots to 0.001 Hz causes a large error in determination of m.

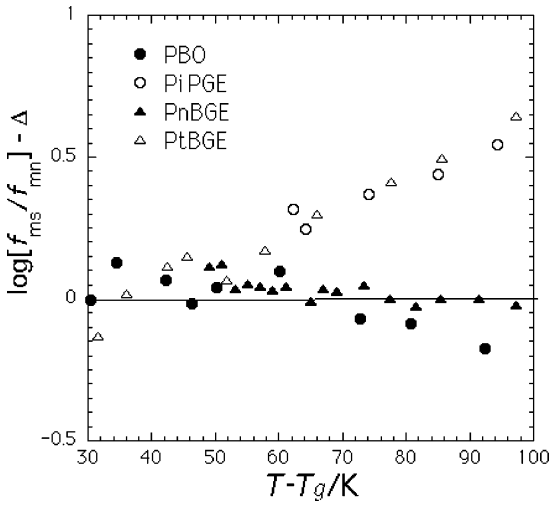

Figure 13. Plots of log(f_{ms}/f_{mn}) vs $T - T_g$. The plots are shifted along the ordinate by $-\Delta$, i.e., $\Delta = 2.46$, 4.70, 4.28, and 4.35 decades for PBO, PiPGE, PnBGE, and PtBGE, respectively.

On the other hand, the values of A and B for the normal mode do not depend much on the chemical structure of the side group. We also note for PBO and PnBGE that B for the normal mode is similar to that for the segmental mode. This indicats that the average relaxation times for the both processes change parallel. For PBO we have already reported this behavior in our previous paper.[16] Casalini and Roland investigated the effects of temperature and pressure on the relationship between the segmental mode and normal mode in PBO. Their results indicate that the relaxation times for the both processes change parallel in the temperature range far above T_g.[15] The same behavior is also known for *cis*-polyisoprene and poly(propylene oxide).[13−15,34,35] Here it is important to note that such discussion is limited to the temperature range of $T > T_g + 30$ K and the frequency range of $f_{ms} > 100$ Hz. Near T_g the separation between log f_{ms} and log f_{mn} decreases with decreasing temperature.[13−15,34−37] In contrast to those behaviors reported previously, it is clearly seen that the average slopes for log f_{ms} of PiPGE and PtBGE are steeper than those for log f_{mn} even in the range of $T > T_g + 30$ K.

To compare the temperature dependences of log(f_{ms}/f_{mn}) among poly(alkyl glycydil ether)s and PBO, log(f_{ms}/f_{mn}) vs $T - T_g$ plots are shown in Figure 13 in which the data for PBO-5 with $M = 4500$ have been used.[16] It is seen that the values of log(f_{ms}/f_{mn}) for PnPGE and PBO are almost independent of T in the range $T > T_g +$ 30 K, but those for PiPGE and PtBGE increase with T. We suspect that the behaviors of PiPGE and PtBGE are due to overestimation of f_{ms} obtained by extrapolation of the Vogel−Fulcher equation. As mentioned above, the segmental mode and the β relaxation merge in the α_s relaxation region. The dynamics of the side group is activated with increasing temperature and enhances the segmental dynamics. Therefore, the temperature dependence of log f_{ms} becomes steeper than ordinary polymers in the α_s relaxation region. If this is the case, the temperature dependence slope of log f_{ms} will become weaker than the extrapolated f_{ms} in the high-temperature region.

Another origin of the temperature dependence of f_{ms}/f_{mn} may be the definition of the average relaxation time. Our interest is in the ratio of the average relaxation time τ_s for the segmental mode and that τ_n for the normal mode. Usually the average relaxation

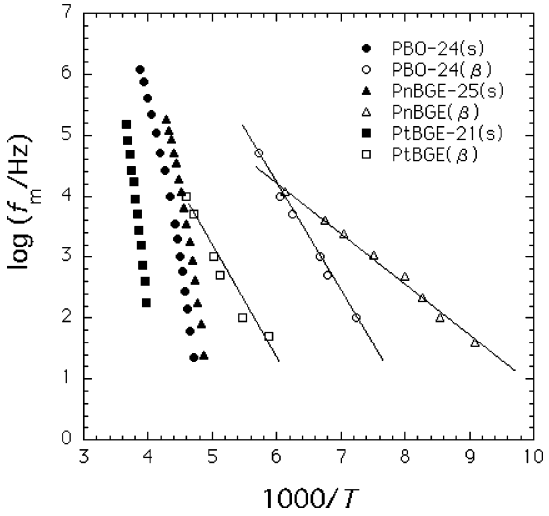

Figure 14. Arrhenius plots of loss maximum frequency f_m for the α_s and β relaxations of PBO, PnBGE, and PtBGE.

Table 4. Activation Energy E_a for the β Relaxation

code	E_a/kJ mol^{-1}	$\Delta\epsilon$
PBO	33.7	0.16
PiPGE (β_1)	28.9	
PiPGE(β_2)	56.3	
PnBGE	15.7	0.30
PtBGE	35.7	0.28

times can be approximated by $1/(2\pi f_m)$, and we assume $\tau_n/\tau_s = f_{ms}/f_{mn}$. However, if the relaxation spectrum for the α_s relaxation is composed of the contributions of segmental motions and rotation of the side group, the value of $1/(2\pi f_m)$ does not become average relaxation time of segmental dynamics. In the present case the shapes of the α_s peaks for PtBGE and PiPGE change with temperature, and hence $1/(2\pi f_m)$ is not equal to τ_s. Thus, $\log(f_{ms}/f_{mn})$ changes with temperature even though the ratio of τ_n/τ_s is independent of temperature.

***β* Relaxation.** We have seen that the intensity of the β relaxation increases with temperature and that the β relaxation merges with the α_s relaxation above T_g. In this section we analyze the β relaxation in detail. Figure 14 shows the Arrhenius plots of f_m for the α_s and β relaxations of PnBGE and PtBGE. For the sake of comparison, those of poly(butylene oxide) (PBO-24) are also plotted.[16] A similar plot for PiPGE has been already shown in Figure 4. We note that the α_s and β relaxations of PnBGE and PtBGE merge around $\log f = 6$ to 7, but it appears that those of PBO do not merge. The Arrhenius plots for the β relaxation conform to a straight line, and the activation energies are listed in Table 4.

Among four polyethers only PBO has a nonpolar side group. Therefore, the β relaxation of PBO cannot be ascribed to rotation of the side group. Casalini and Roland reported that the loss curve for the α relaxation exhibits an excess wing in the high-frequency side.[15] The secondary process may correspond to the β relaxation observed in the present study. They found that the secondary loss peak locates much higher frequency than expected for the Johari−Goldstein process and depends weakly on temperature.[38] Therefore, the β relaxation of PBO cannot be assigned to the Johari−Goldstein process and is assigned to local twisting motions of the main chain proposed by Ishida and Yamafuji.[39] As seen in Figure 14, the behavior of the β relaxation of PBO is similar to that of poly(alkyl glycidyl ether)s. Therefore, we speculate that the β relaxation in poly(glycidyl ether)s is partly due to local twisting motions of the main chain but mainly due to libration of the side groups. Splitting of the β relaxation in PiPGE may be due to decoupling of both relaxations.

Merging of the α and β relaxations has been investigated by many authors with a special interest in the Johari−Goldstein mode.[40−43] It was reported that the Arrhenius plot for the Johari−Goldstein process does not conform to a straight line.[41,42] For the β relaxation as in the present poly(alkyl glycidyl ether)s merging behavior has been reported for various polymers.[44]

The frequency dependence curve in the β region is broad, and hence the relaxation strength $\Delta\epsilon$ for the β relaxation cannot be determined from the Cole−Cole plot. Therefore, the temperature dependence curve was employed to determine $\Delta\epsilon$:[44]

$$\Delta\epsilon = \frac{2E_a}{\pi R}\int_{-\infty}^{\infty}\epsilon''\,\mathrm{d}(1/T) \tag{5}$$

where E_a is the activation energy, R the gas constant, and ϵ'' the loss measured at constant frequency f. Thus, calculated $\Delta\epsilon$ at $f = 100$ Hz are listed in Table 4. For PiPGE $\Delta\epsilon$ was not determined since it was difficult to resolve the β_1 and β_2 peaks. Obviously, the side group is not rotating fully in the glassy state and only librates in a small amplitude. As mentioned above, the amplitude of libration increases with temperature and the side groups rotate almost fully in the temperature range where the α_s relaxation is observed at 1−10 MHz.

It is well-known that some polymers having flexible side groups such as syndiotactic poly(methyl methacrylate) (PMMA) exhibit clear decoupling of motions of the side group and segments.[44] On the other hand, some polymers such as poly(vinyl acetate) (PVAc) do not exhibit such dynamical heterogeneity.[44] Poly(alkyl glycidyl ether)s exhibit intermediate behavior; i.e., at low temperature the motions of the side group and the backbone are decoupled, but above T_g they are coupled. Those behaviors may be related to the phenomena of dynamical heterogeneity in miscible polymer blends in which distinct dynamics of the components is observed.[20] The relationship between the mobility of the side groups and segments is an interesting future issue.

Conclusion

Poly(isopropyl glycidyl ether) (PiPGE), poly(*n*-butyl glycidyl ether) (PnBGE), and poly(*t* -butyl glycidyl ether) (PtBGE) exhibit three dielectric relaxations designated as α_n, α_s, and β from the high-temperature side. The α_n relaxation is assigned to the normal mode relaxation due to fluctuation of the end-to-end vector. The α_s relaxation is observed about 20−30 K above the glass transition temperature T_g and is assigned to the primary relaxation. The β relaxation is observed below T_g and is due to both the twisting motions of the backbone of the chains and the libration of the side groups. The intensity of the β relaxation is very low in the low temperature but increases with increasing temperature. The Arrhenius plots of the loss maximum frequency f_m indicate that the α_s and β relaxations merge above T_g. Therefore, the α_s relaxation is due to both local segmental motion and rotation of side groups. The relaxation strengths for the segmental mode $\Delta\epsilon_s$ and those for the normal mode $\Delta\epsilon_n$ have been determined by using the Cole−Cole plots. For the α_s relaxation, the value of

$g^{1/2}p_B$ is determined where g is the Kirkwood dipole−dipole correlation factor and p_B the dipole moment. The factor g is found to be less than unity. From the relaxation strength $\Delta\epsilon_n$ for the α_n relaxation, the parallel dipole moment p_A per unit contour length has been determined. The parallel dipole moments of poly(alkyl glycidyl ether)s are smaller than that of PBO having nonpolar side group. Thus, the parallel dipole moment depends strongly on the electronic affinity of the side groups which results in the asymmetry of the electronic density in the C−O−C bond. The loss maximum frequency f_{ms} for the α_s relaxation and that f_{mn} for the α_n relaxation conform to the Vogel−Fulcher equation. The average slopes of the f_{mn} vs $1/T$ plots for PiPGE and PtBGE are higher than those of PBO and PnBGE. We have examined the temperature dependence of $\log(f_{ms}/f_{mn})$ using f_{ms} estimated by extrapolation with the Vogel −Fulcher equation and found that $\log(f_{ms}/f_{mn})$ is almost independent of temperature for PBO and PnBGE, but those for PiPGE and PtBGE increase with temperature.

References and Notes

(1) Stockmayer, W. H. *Pure Appl. Chem.* **1967**, *15*, 539.
(2) Adachi, K.; Kotaka, T. *Prog. Polym. Sci.* **1993**, *16*, 585.
(3) Dielectric Properties of Amorphous Polymers In *Dielectric Spectroscopy of Polymeric Materials*; Runt, J. P., Fitzgerald, J. J., Eds.; American Chemical Society: Washington, DC, 1997.
(4) *Broadband Dielectric Spectroscopy*; Kremer, F., Schönhals, A., Eds.; Springer: New York, 2002.
(5) Watanabe, H. *Prog. Polym. Sci.* **1999**, *24*, 1253.
(6) Diaz-Calleja, R.; Compan, V.; Riande, E. *Physica B* **2004**, *349*, 371.
(7) Baur, M. E.; Stockmayer, W. H. *J. Chem. Phys.* **1965**, *43*, 4319.
(8) Schlosser, E.; Schonhals, A. *Prog. Colloid Polym. Sci.* **1993**, *91*, 158.
(9) Schonhals, A.; Kremer, F. *J. Non-Cryst. Solids* **1994**, *172−174*, 336.
(10) Hayakawa, T.; Adachi, K. *Polymer* **2001**, *42*, 1725.
(11) Kyritsis, A.; Pissis, P.; Mai, S.-M.; Booth, C. *Macromolecules* **2000**, *33*, 4581.
(12) Fragiadakis, D.; Bouga, M.; Kyritsis, A.; Pissis, P.; Viras, K.; Mingvanish, W. S. M.; Booth, C. *Macromol. Sympo* **2003**, *191*, 21.
(13) Roland, C. M.; Psurek, T.; Pawlus, S.; Paluch, M. *J. Polym. Sci., Part B: Polym. Phys.* **2003**, *41*, 3047.
(14) Roland, C. M.; Paluch, M.; Casalini, R. *J. Polym. Sci., Part B: Polym. Phys.* **2004**, *42*, 4313.
(15) Casalini, R.; Roland, C. M. *Macromolecules* **2005**, *38*, 1779.
(16) Yamane, M.; Hirose, Y.; Adachi, K. *Macromolecules* **2005**, *38*, 9210.
(17) Hirose, Y.; Adachi, K. *Polymer* **2005**, *46*, 1913.
(18) Uzaki, S.; Adachi, K.; Kotaka, T. *Macromolecules* **1988**, *21*, 153.
(19) Uzaki, S.; Adachi, K.; Kotaka, T. *Polymer* **1988**, *20*, 221.
(20) Haley, J. C.; Lodge, T. P.; He, Y.; Ediger, M. D.; von Meerwall, E. D.; Mijovic, J. *Macromolecules* **2003**, *36*, 6142 and references cited therein.
(21) Stolarzewich, A.; Neugebauer, D. *Macromol. Chem. Phys.* **1999**, *200*, 2467.
(22) Imanishi, Y.; Adachi, K.; Kotaka, T. *J. Chem. Phys.* **1988**, *89*, 7585.
(23) Rouse, P. E. *J. Chem. Phys.*. **1953**, *21*, 1272.
(24) De Gennes, P. G. *J. Chem. Phys.* **1971**, *55*, 572.
(25) Doi, M.; Edwards, S. F. *J. Chem. Soc., Faraday Trans. 2* **1978**, *74*, 1789, 1802, 1818.
(26) Onsager, L. *J. Am. Cem. Soc.* **1936**, *58*, 1486.
(27) Kirkwood, J. G. *J. Chem. Phys.* **1939**, *7*, 911.
(28) Matsushima, M.; Fukatsu, M.; Kurata, M. *Bull. Chem. Soc. Jpn.* **1968**, *41*, 2570.
(29) Brandrup, J.; Immergut, E. H. *Polymer Handbook*, 3rd ed.; John Wiley & Sons: New York, 1989.
(30) Vogel, H. *Phys. Z.* **1921**, *22*, 645.
(31) Fulcher, J. G. *J. Am. Ceram. Soc.* **1925**, *8*, 339.
(32) Hayakawa, T.; Adachi, K. *Polym. J.* **2000**, *32*, 845.
(33) Bohmer, R.; Ngai, K. L.; Angell, C. A.; Plazek, D. J. *J. Chem. Phys.* **1993**, *99*, 4201.
(34) Schönhals, A. Dielectric Properties of Amorphous Polymers. In *Dielectric Spectroscopy of Polymeric Materials*; Runt, J. P., Fitzgerald, J. J., Eds.; American Chemical Society: Washington, DC, 1997; pp 81−106.
(35) Adachi, K.; Hirano, H. *Macromolecules* **1998**, *31*, 3958.
(36) He, Y.; Lutz, T. R.; Ediger, M. D. *Macromolecules* **2004**, *37*, 9889.
(37) Roland, C. M.; Ngai, K. L.; Santangelo, P. G.; Qui, X. H.; Ediger, M. D.; Plazek, D. J. *Macromolecules* **2001**, *34*, 6159.
(38) Johari, G. P.; Goldstein, M. *J. Chem. Phys.* **1972**, *55*, 4245.
(39) Ishida, Y.; Yamafuji, K. *Kolloid Z.* **1961**, *176*, 62.
(40) Ngai, K. L.; Paluch, M. *J. Chem. Phys.* **2004**, *120*, 857.
(41) Fujima, T.; Furusawa, H.; Ito, K. *Phys. Rev. E* **2002**, *66*, 031503.
(42) Nozaki, R.; Suzuki, D.; Ozawa, S.; Shiozaki, Y. *J. Non-Cryst. Solids* **1998**, *235−237*, 393.
(43) Roland, C. M.; Schroeder, M. J.; Fontanrlla, J. J.; Ngai, K. L. *Macromolecules* **2004**, *37*, 2630.
(44) McCrum, N. G.; Read, B. E.; Williams, G. *Anelastic and Dielectric Effects in Polymeric Solids*; John Wiley & Sons: New York, 1967, and Dover Publications Inc.: New York, 1991.

MA051796V